

# Polymerization from the Vapor Phase. I. Poly(*p*-phenyleneterephthalamide) Gas Barrier Coatings

R. M. IKEDA, R. J. ANGELO, F. P. BOETTCHER, R. N. BLOMBERG, and  
M. R. SAMUELS, *E. I. du Pont de Nemours and Company, Inc.*,  
*Experimental Station, Wilmington, Delaware 19898*

## Synopsis

An atmospheric-pressure, vapor-phase polymerization technique was used to deposit thin (1–10  $\mu\text{m}$ ) poly(*p*-phenyleneterephthalamide) coatings onto polyester film and other sheet substrates. A minimum deposition temperature of 170°C was found to be critical. When substrate temperatures were below 170°C, coatings were loosely adhered, powdery, and of low molecular weight; above 170°C, coherent, well-adhered, high molecular weight coatings were obtained. These vapor-deposited coatings exhibited exceptionally good oxygen barrier properties and were found to consist of fused 0.1- $\mu\text{m}$  particulates. Scanning electron microscopy (SEM) of the top surfaces of these coatings clearly revealed their particulate origin. Similar evidence was also obtained from SEM examination of fracture surfaces and transmission electron microscopy of microtomed sections. The coalescence of these coatings was demonstrated by SEM of plasma-etched surfaces and oxygen permeability information. The uniplanar orientation of the polymer crystals in these multiparticulate coatings was strong evidence for the epitaxial growth of the crystals.

## INTRODUCTION

A solventless polymerization<sup>1</sup> and deposition<sup>2</sup> technique was found that permits the direct formation of thin (1–10  $\mu\text{m}$ ) poly(*p*-phenyleneterephthalamide) (PPD-T) coatings from the vaporized monomers *p*-phenylenediamine (PPD) and terephthaloyl chloride (TCL). The vapor-deposited PPD-T coatings were unexpectedly good oxygen barriers that were relatively unaffected by exposure to moisture. Permeability coefficients ( $0.32 \times 10^{-13}$  cc(S.T.P.) cm/cm<sup>2</sup> sec cm Hg) were 1000 times lower than those measured for similar PPD-T coatings applied by solution techniques.

Depending on the polymerization conditions, the PPD-T deposits were either powdery or coherent. Powdery coatings were deposited when the substrate temperatures were below  $\sim 170^\circ\text{C}$ . Above 170°C, coherent coatings were formed, but the coatings were either clear or hazy depending on the monomer flow rates. At flow rates greater than about 1 mmol/min hazy coatings were formed. The vapor-deposited PPD-T coatings were slightly yellow, whereas their solution-deposited counterparts tended to be clear, colorless, and coherent.

## EXPERIMENTAL

### Apparatus and Polymerization Conditions

The equipment used for the vapor-phase reactions was constructed from 316 stainless steel and is illustrated schematically in Figure 1.

**Monomers and Monomer Storage.** Polymerization-grade terephthaloyl

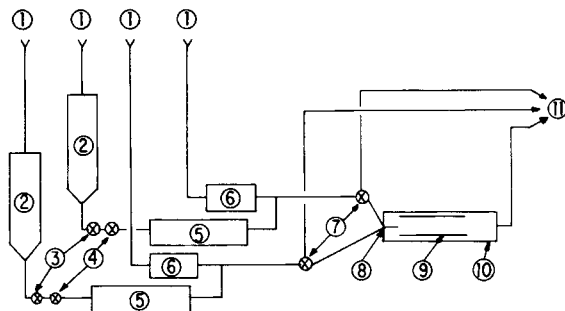


Fig. 1. Apparatus schematic: (1) dry  $N_2$  source; (2) liquid monomer storage containers; (3) metering valves; (4) calibration dump valves; (5) vaporizers; (6)  $N_2$  heaters; (7) bypass valves; (8) reactor "Y" (9) film substrate; (10) reactor; (11) cyclone, bag collector, and water scrubber.

chloride (TCl) and *p*-phenylenediamine (PPD) were obtained from the Organic Chemicals Department of the du Pont Company and used without further purification. The monomers were stored as liquids ( $126^\circ\text{C}$  for TCl and  $165^\circ\text{C}$  for PPD) in 2-liter stainless steel containers under 40 psi dry nitrogen.

**Monomer Feed.** Liquid monomers were metered into the vaporizers by the pressure drop across a fine double-needle valve (Nupro double-pattern metering valve SS-2MGD). Flow rates (0.5 to 5 mmol/min) were measured by using a three-way valve to dump the output from the metering valve directly into a weighing dish and by calibrating over an appropriate time period (1–10 min).

**Monomer Vaporization.** Vaporizers consisted of 2-ft sections of  $\frac{3}{8}$ -in.-i.d. Inconel pipe electrically heated to  $320$ – $350^\circ\text{C}$ . Initially, a small flow [0.5–5 standard cubic feet per hour (SCFH)] of preheated  $320^\circ\text{C}$  nitrogen was used to purge the vaporizers and to ensure steady vapor delivery to the carrier gas. No effect on the deposition rates was noted with or without this purge, and it was discontinued in later runs.

**Carrier Gas.** Before mixing with the vaporized monomers, the nitrogen carrier gas was metered through Brooks rotameters and electrically heated to the desired temperature ( $100$ – $300^\circ\text{C}$ ). Typically the nitrogen temperature was  $180^\circ\text{C}$ , with a flow of 20–100 SCFH for each monomer. Monomer gas concentrations were 0.05–1%. Most experiments were carried out at about 0.1% monomer concentrations and 50 SCFH nitrogen flow per monomer.

**Reactor.** The electrically heated reactor was a 14-in. section of thin-walled (0.060-in.) 2-in.-o.d. stainless steel tubing. The two monomer vapor streams were mixed at one end of the reactor at a "Y" constructed from  $\frac{3}{8}$ -in.-o.d. stainless steel tubing. Polymer was deposited onto 6 × 6-in. substrate sheets that were taped on aluminum foil fitted tightly around the interior circumference of the reactor. Substrate temperatures were typically  $170$ – $200^\circ\text{C}$ , but temperatures as high as  $310^\circ\text{C}$  and as low as  $8^\circ\text{C}$  were employed. Three-way valves permitted bypassing the reactor for changing and preheating the substrates. Typical coating experiments lasted from 0.5 to 30 min to obtain coatings 1–10  $\mu\text{m}$  thick.

**Waste Treatment.** The hot gases exiting or bypassing the reactor were quenched in cold nitrogen gas. Particulate matter was separated by a cyclone and collected in a felt bag of Nomex aramid felt. Exit gases were run through a water scrubber and vented into an exhaust hood.

### Substrates

Sheet substrates, 6 × 6 in., were used in the coating experiments discussed here. In most cases, biaxially oriented poly(ethyleneterephthalate) (PET) sheets 50 μm thick were used as the substrate of choice, but aluminum foil and polyimide film were also employed. In general, any substrate that could withstand the 170–200°C coating environment could be used.

### Solution Coating

For comparison purposes, high molecular weight PPD-T prepared in hexamethylphosphoramide solvent<sup>3</sup> was applied onto oriented PET substrates by solvent coating. Dilute solutions (2%) of the polymer in concentrated sulfuric acid were cast directly onto PET film using a Meyer rod. Coated samples were quickly immersed in ice water to form a gel coating that was neutralized by soaking in dilute NaHCO<sub>3</sub>. Drying was carried out in a vacuum oven at 125°C overnight with a nitrogen bleed.

### Coating Characterization

**Coating Thickness.** Average coating thicknesses were calculated from accurately determined coating weights (±1 mg) and substrate areas. A polymer density of 1.45 g/cc was assumed in the thickness calculation.

**Sample Isolation.** Usually, the coatings adhered tenaciously to the PET substrates but could be stripped from polyimide and aluminum foil surfaces. A variety of polymer isolation techniques were tried, but the most satisfactory method employed coatings deposited onto aluminum foil. The aluminum foil was dissolved in hydrochloric acid (~5*N*) leaving flakes of the insoluble polymeric coating. The polymer flakes were then washed thoroughly with water and vacuum dried. When the coatings were lifted directly from the polyimide or aluminum foil sheets, they were washed in water (plus detergent) to remove the static electricity before drying in a vacuum oven.

**Density.** A carbon tetrachloride–hexane density gradient tube (ASTM D1505) was used for density measurements. Data are summarized in Table I. In general, the vapor-phase-deposited PPD-T coatings prepared at 170–200°C exhibited densities of ≥1.46 g/cc. At higher deposition temperatures, >230°C, coatings of somewhat lower density were formed. The densities of the PPD-T coatings deposited from dilute sulfuric acid solution were about 1.40 g/cc.

**Inherent Viscosity—Molecular Weight.** Inherent viscosity ( $\eta_{inh}$ ) measurements at 0.5% concentration in 100% sulfuric acid were made at 30°C. The solution viscosity values were converted to molecular weights by the equation

$$\eta_{inh} = 1.17 \times 10^{-3} \bar{M}_n^{0.846} \quad (1)$$

determined by F. B. Moody<sup>4</sup> by endgroup analysis.

**Oxygen Permeability.** The oxygen permeabilities of coated films were measured using the Mocon Oxtran 100 instrument. Although the coated samples were measured at 27°C and 80% RH, the 1–2 hr of exposure during measurement was not sufficient to establish moisture equilibrium, and the measurements were considered to be done under ambient conditions.

The following expression was used to calculate the permeability of the coating

TABLE I  
Densities and Inherent Viscosities of PPD-T Coatings. Vapor-Phase-Deposited Coatings

No.	Substrate	Deposition temp., °C	$\eta_{inh}^a$ , dl/g	Density, <sup>b</sup> g/cc
139-4	Al foil	168	2.26	1.461 <sub>0</sub>
35C	Al foil	170	2.07	1.466 <sub>2</sub>
23-4	polyamide	190	2.76	1.466 <sub>8</sub>
86-0	Al foil	190	2.50	1.465 <sub>6</sub>
103-0	Al foil	200	2.73	1.462 <sub>6</sub>
14	Al foil	232	2.82	1.465
14-14	polyamide	232	—	1.462 <sub>6</sub>
86	Al foil	232	3.08	1.452 <sub>0</sub>
18	Al foil	244	2.42	1.461 <sub>0</sub>
88	Al foil	270	2.54	1.454 <sub>0</sub>
92	Al foil	320	3.42	1.427 <sub>6</sub>
Coatings from 2% H <sub>2</sub> SO <sub>4</sub> Solutions				
96-2	—	25	3.61	1.398 <sub>8</sub>
96-20	—	25	—	1.398 <sub>6</sub>
164	—	25	—	1.340
164	—	25	—	1.402

<sup>a</sup> 0.5% in conc. H<sub>2</sub>SO<sub>4</sub> at 30°C.

<sup>b</sup> Density gradient tube.

from measurements on the coated films:

$$\frac{1}{P_c} = \frac{1}{P_a} + \frac{1}{P_b} \quad (2)$$

The subscript *c* indicates the coated film, *a* the base film, and *b* the coating. Assuming a linear permeability–thickness relationship, the permeability of the coating per unit thickness was calculated from the following:

$$P_b = p_b \times \text{thickness} \quad (3)$$

where *p<sub>b</sub>* is the permeability per unit thickness of coating. In this report, permeabilities are listed in the ASTM unit, barrier (*B*) (10<sup>10</sup> × cc(S.T.P.)-cm/cm<sup>2</sup> sec cm Hg). The prefixes milli- and kilo- are also used indicating 0.001× and 1000×, respectively.

**Water Vapor Transmission.** Water vapor transmission rates were measured by a cup technique, ASTM-E96 procedure E. Coated substrates were measured with the coating side exposed to high humidity conditions (38°C, 90% RH), and the water vapor permeability of the coating was calculated from eq. (2), as described above.

**Microscopy.** A Leitz Ortholux Research optical microscope was used to examine the powdery deposits and clear coatings. For cross section observations, specimens were potted in a two-part epoxy resin (from Specialty Plastic Co., Inc., Baltimore, Maryland), microtomed to 50 nm using a Porter–Blum MT2 ultramicrotome and examined with a Phillips 200 electron microscope. Samples were also examined by a JEOL JSM-15 scanning electron microscope after vapor depositing a standard Au–Pd conductive coating onto the specimens.

**Wide-Angle X-Ray Measurements.** These include 2θ goniometer scans

made on isolated coating chips. Flat-plate photographs were made using a standard flat-plate camera with a 5-cm sample-film distance and copper  $K\alpha$  radiation. In some x-ray experiments, flat-plate photographs were taken with the coating chips perpendicular to the beam and at  $45^\circ$  to the beam.

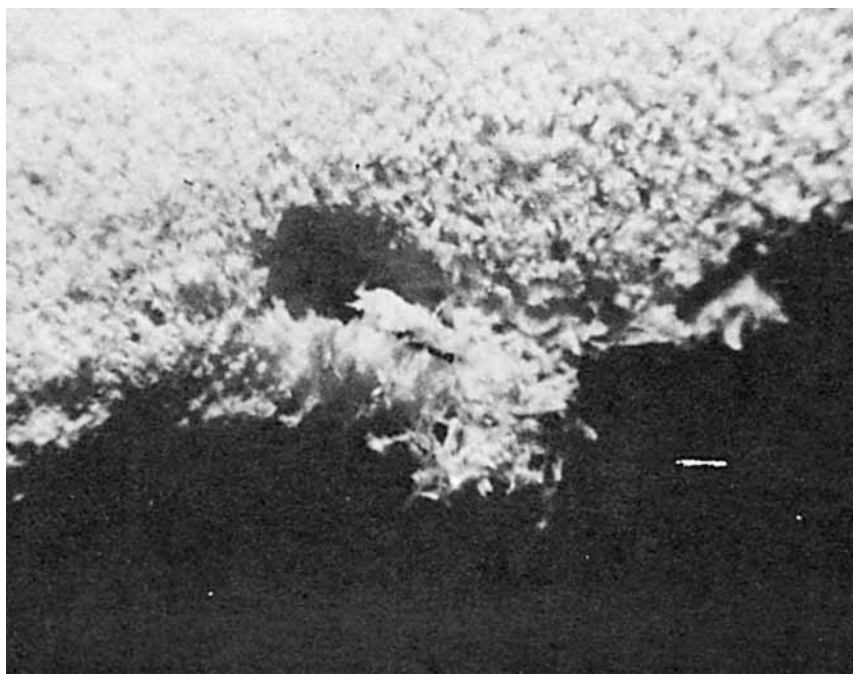
## RESULTS AND DISCUSSION

Our initial experiments showed that the appearance and the character of the deposits formed by the direct vapor-phase reaction of PPD and TCl were strongly affected by the substrate temperatures. Preparations were made with substrate temperatures ranging from 8 to  $310^\circ\text{C}$ . Below  $170^\circ\text{C}$  the deposits were powdery and loosely adhered [Fig. 2(a)]. Above  $170^\circ\text{C}$  the coating character changed completely. The deposits were coherent (optical microscopy at  $50\times$ ) and well adhered to the PET substrates [Fig. 2(b)]. The data in Table I and Figure 3 also demonstrate the strong effect of deposition temperature on the coating inherent viscosity. Below  $170^\circ\text{C}$  the deposit inherent viscosity is constant at about 1 (degree of polymerization  $\cong 10$ ). Above  $170^\circ\text{C}$  the inherent viscosity increases with reaction temperature. Other experiments indicated that the inherent viscosity was rather insensitive to all other process variables. Reaction times from 10 sec to 2 hr were tried without the marked change in inherent viscosity. Monomer concentrations and ratios, substrate variations, and reactor geometries were also varied without observing a very strong effect on the deposit molecular weight.

With a reactor temperature of  $200\text{--}210^\circ\text{C}$ , the typical inherent viscosity of the deposit was 2.5. This indicates a polymer molecular weight of 8700 or a degree of polymerization of  $\sim 36$ . While this molecular weight is not high, it is obvious that the vapor deposits are definitely polymeric. The composition of the polymers was examined by infrared spectroscopy. The infrared spectrum of the vapor-deposited coatings was compared with that obtained from a PPD-T sample prepared in solution<sup>3</sup> and made into a coating by casting from dilute sulfuric acid. Except for slight differences in intensity, attributable to thickness differences, the spectra were identical. We thus concluded that the well-coalesced deposits formed by the vapor-phase reaction of *p*-phenylenediamine and terephthaloyl chloride were indeed poly(*p*-phenyleneterephthalamide) as we had expected.

The coherent, well-adhered, vapor-phase-deposited PPD-T coatings were sometimes clear and shiny and at other times dull and hazy. The coating appearance was related to material flow as illustrated in Figure 4. Other variables such as the deposition temperatures ( $170\text{--}300^\circ\text{C}$ ), the monomer ratios, etc. did not influence the coating appearance. While the details of this relationship may be specific to PPD-T and to the peculiarities of our reactor configuration, it does appear that the hazy coatings are definitely associated with high total monomer delivery at the reactor.

Oxygen permeability data for representative clear coatings of vapor-deposited PPD-T are shown in Table II. The consistency of the calculated coating permeability indicates an inverse relationship between the coating thickness and its permeability. This implies that the barrier is a bulk property of the coating and not some unusual surface phenomenon. The average oxygen permeability value is quite low,  $0.032 \pm 0.017$  millibarriers (mB). This value is compared with



(a)



(b)

Fig. 2. Deposits from gaseous *p*-phenylenediamine and terephthaloyl chloride observed in an optical microscope at low magnification (25X): (a) powdery deposit made at 25°C; (b) coalesced deposit made at 200°C.

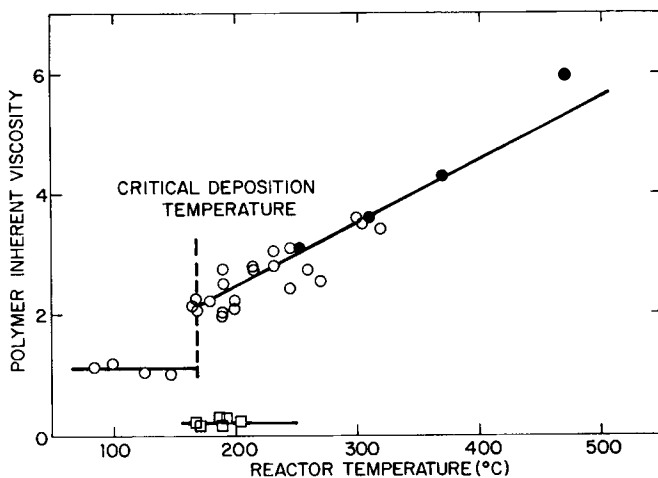


Fig. 3. Polymer viscosity change with reactor temperature. Open circles represent material collected from the substrates in the reactor. Filled circles represent literature data<sup>1</sup> collected under similar circumstances. Squares represent data obtained on material that passed through the reactor at the specified temperature and subsequently collected in the particle separator and bag collector.

the oxygen permeability for several organic polymeric materials in Table III. You will note that its barrier to oxygen is significantly better than that for polyacrylonitrile and poly(vinylidenechloride), both known as high barrier materials. It is also significant to note that the vapor-deposited coating has an oxygen permeability 100 times lower than that of a solution-prepared coating. X-Ray characterization of both the vapor-deposited and solution-deposited coatings indicated a high degree of crystallinity in both cases, but a careful quantitative study that might shed light on the large differences in the permeability of these two samples was not conducted. At this time, we may only conclude that the similarity of the x-ray traces precludes a simple crystallinity

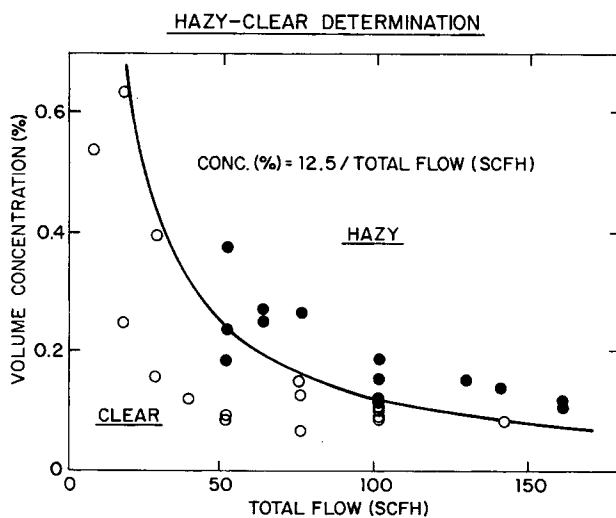


Fig. 4. Monomer concentration/flow dependence of hazy/clear deposits.

TABLE II  
Representative Oxygen Permeabilities for Clear VPP PPD-T Coatings

No.	Thickness, $\mu\text{m}$	$P_c(\text{O}_2)/\text{cm},^a$ B/cm	$P_c(\text{O}_2),^b$ mB
1683	0.8	0.49 <sub>6</sub>	0.04 <sub>4</sub>
1686	1.0	0.30 <sub>7</sub>	0.03 <sub>2</sub>
717-4	1.0	0.26 <sub>0</sub>	0.02 <sub>7</sub>
174-6	2.0	0.18 <sub>9</sub>	0.03 <sub>8</sub>
125-2	2.1	0.11 <sub>8</sub>	0.02 <sub>5</sub>
139-1	2.1	0.11 <sub>8</sub>	0.02 <sub>5</sub>
139-6	3.0	0.09 <sub>4</sub>	0.02 <sub>9</sub>
168-1	3.0	0.14 <sub>2</sub>	0.04 <sub>4</sub>
716-7	3.3	0.09 <sub>4</sub>	0.03 <sub>2</sub>
168-4	3.0	0.23 <sub>6</sub>	0.08 <sub>9</sub>
713-2	4.1	0.07 <sub>1</sub>	0.02 <sub>9</sub>
716-6	4.1	0.07 <sub>1</sub>	0.02 <sub>9</sub>
717-6	4.6	0.02 <sub>4</sub>	0.01 <sub>1</sub>
718-3	4.6	0.04 <sub>7</sub>	0.02 <sub>2</sub>
716-4	4.6	0.02 <sub>4</sub>	0.01 <sub>1</sub>
716-5	5.6	0.04 <sub>7</sub>	0.02 <sub>6</sub>
713-4	9.6	0.02 <sub>4</sub>	0.02 <sub>3</sub>
			(0.03 <sub>2</sub> $\pm$ 0.01 <sub>7</sub> )

<sup>a</sup> Units: ( $10^{10} \times \text{cc}(\text{S.T.P.}) - \text{cm}/\text{cm}^2 - \text{sec} - \text{cm Hg}$ )/cm.

<sup>b</sup> Units: ( $10^{13} \times \text{cc}(\text{S.T.P.}) - \text{cm}/\text{cm}^2 - \text{sec} - \text{cm Hg}$ ).

argument to explain either the permeability data or the density differences shown in Table I.

The oxygen permeability data for the hazy coatings are also given in Table III. They are about three times greater than those for the clear coatings and vary quite markedly.

Hydrogen-bonded polymers (i.e., nylon 66, cellulose, Nomex, etc.) are known to have good gas barriers when dry, but the barrier usually degrades with water uptake.<sup>5</sup> The effect of humidity on the vapor-phase-prepared PPD-T coatings was first studied by exposing coated films to 100% RH at 22°C and periodically

TABLE III  
Barrier Properties of VPP PPD-T and Other Polymer Films

	$P_b(\text{O}_2),^a$ mB	$P_b(\text{H}_2\text{O}),^b$ B
Clear VPP PPD-T	0.03 $\pm$ 0.017	14.8 $\pm$ 11.6
Hazy VPP PPD-T	0.100 $\pm$ 0.056	—
Soln.-deposited PPD-T	3.8 $\pm$ 1.6	108 $\pm$ 84
Polyacrylonitrile	0.18–0.24	360
Poly(vinylidene chloride)	0.24–1.2	1.2–3.0
LOPAC (AN/S)	3.6	400
Saran	4.2	26
Kel-F	18	28
100A Mylar polyester film	30	210
Low-density polyethylene	540	32

<sup>a</sup> Units: ( $10^{13} \times \text{cc}(\text{S.T.P.}) - \text{cm}/\text{cm}^2 - \text{sec} - \text{cm Hg}$ ).

<sup>b</sup> Units: ( $10^{10} \times \text{cc}(\text{S.T.P.}) - \text{cm}/\text{cm}^2 - \text{sec} - \text{cm Hg}$ ).



monitoring their oxygen permeability. After two weeks at 100% RH, equilibrium occurred and the oxygen permeabilities were two to five times their original value. Samples were also exposed to dry steam conditions (150°C, 60 sec, 1 atm) and wet steam condition (115°C, 15 min, 10 psig). The oxygen permeabilities were found to double by these treatments. The relative insensitivity of the oxygen permeability of this polyamide coating might be associated to the low solubility of water in the polymer. A differential scanning calorimetric technique was used to determine the quantity of water in the coatings after being exposed to 50% RH and 22°C. The dilute solution-cast sample was found to have a 4.5% moisture content, whereas the vapor-phase-prepared sample contained considerably less water, 0.7%.

While the optical examination of the clear coating surface (Fig. 2) appeared to show a well-adhered smooth coating, examination of the same surfaces with electron microscopy indicated a highly textured surface. This is illustrated by the scanning electron micrograph of Figure 5 and also in the replica observed by transmission electron microscopy in Figure 6. Fifty to 60 different preparations were examined by scanning electron microscopy, and in all cases the top surface appeared to be composed of particulates with dimensions on the order of 0.1  $\mu\text{m}$ . The bottom surfaces of the deposits were always smooth, and oxygen plasma etching studies as well as the linear dependence of the permeability with reciprocal thickness indicated a well-coalesced interior of the coating. The top surface of the solution-coated samples with their 100 times greater oxygen permeability was always smooth at this magnification (10,000 $\times$ ).

In Figure 1(b) a probe was pushed along the surface of the coating, and the

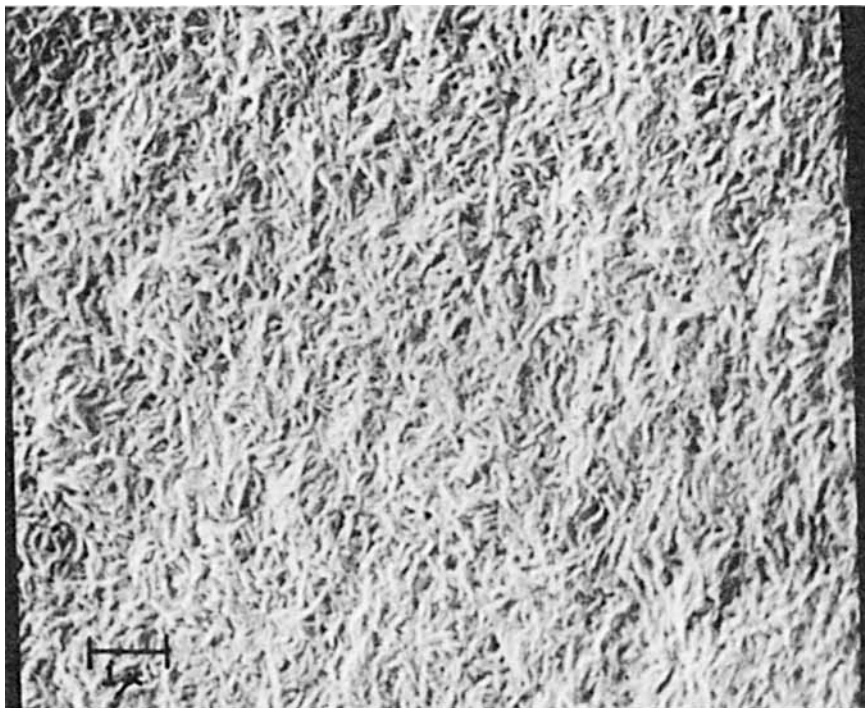


Fig. 5. Scanning electron micrograph of a clear, coalesced deposit made at 200°C. Particulate dimensions are on the order of 0.1  $\mu\text{m}$ .

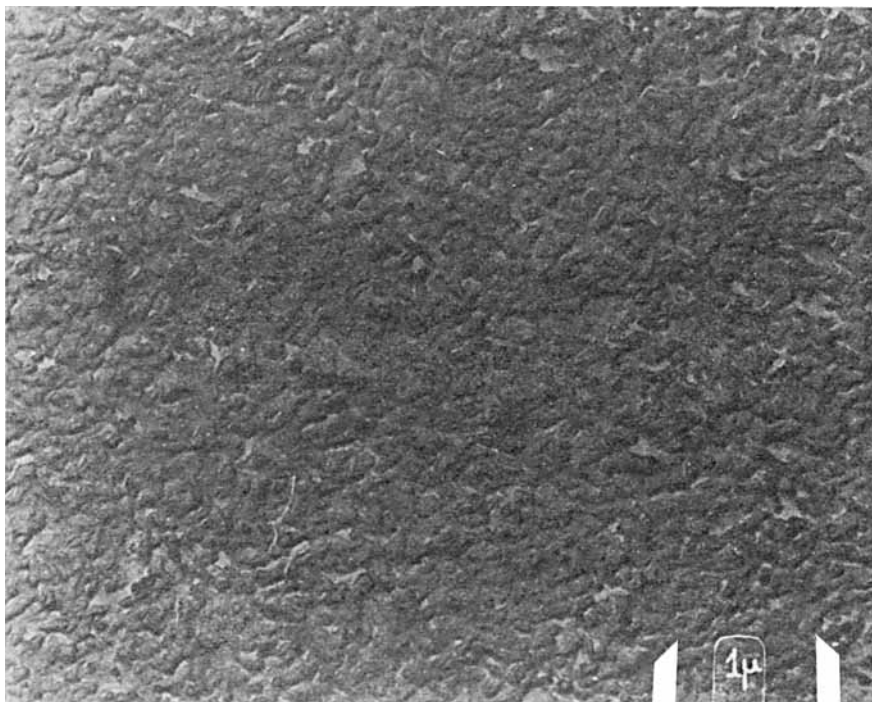


Fig. 6. Transmission electron micrograph of a carbon replica of a clear, coalesced deposit made at 200°C.

resulting gouged polymer led one to believe that the coating might be quite ductile or waxy. To further investigate this possible ductility, vapor-phase-coated polyester films were stretched in an Instron tensile tester to 1, 2, and 5% elongation. When the coatings were examined, cracks were found perpendicular to the stretch direction at elongations of only 1–2%. The deposits thus appeared to be quite brittle on a macroscopic scale. Scanning electron micrographs of these fractured surfaces again revealed the particulate origin of the deposits. This is seen in Figure 7. Although well coalesced, the integrity of the individual particulates was still maintained, and their deformation in the fracture surface again gave some indication of possible ductility. Similar ductility was also encountered in the difficulty in microtoming the coatings. Microtome cross sections (Fig. 8) always revealed asymmetric particulates with their short dimensions parallel to the cutting direction of the knife and independent of the orientation of the coating. This particulate distortion again appeared to imply a basic ductility of the particles.

Another noteworthy characteristic of these vapor-deposited PPD-T coatings was the orientation of the polymer crystal. X-ray goniometer traces and flat-plate photographs both indicated that the coatings were highly crystalline, but the  $2\theta$  values of the strongest reflection were different in each experiment. The goniometer traces showed a very strong (110) reflection,<sup>2</sup> while the flat-plate photographs revealed a strong (020) reflection. These x-ray results were compatible with an oriented coating. The x-ray beam in the goniometer was essentially parallel to the deposit surface, while in the flat-plate camera the beam was perpendicular to the surface. A crystal orientation with the (100) planes

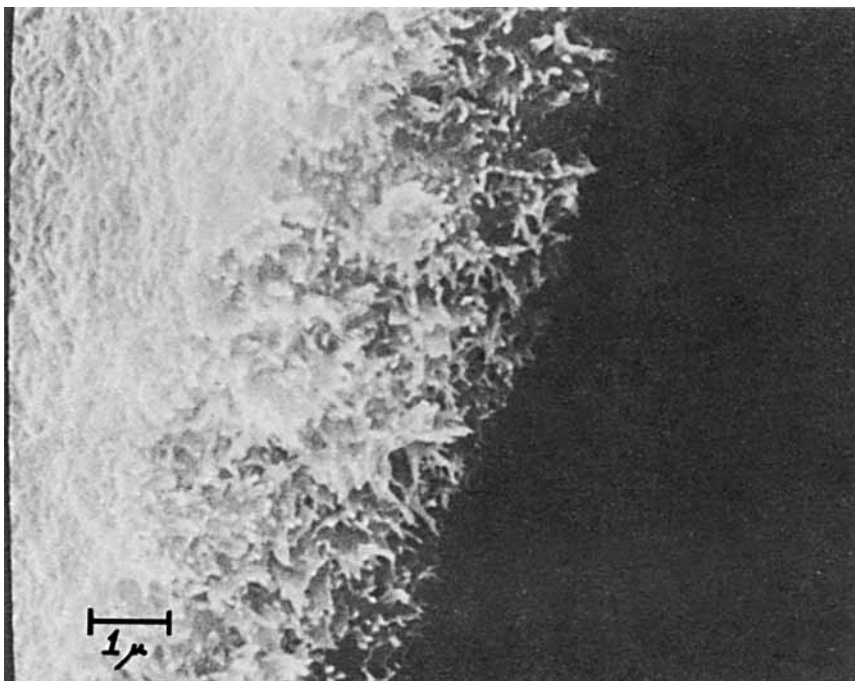


Fig. 7. Scanning electron micrograph of a fracture surface of a clear deposit made at 190°C. The fracture was obtained at 25°C using a slow, tensile deformation.

parallel to the substrate-coating interface would give these results. This conclusion was confirmed by other flat-plate camera experiments where the coating chips were first placed perpendicular to the beam and then tilted 45° to the beam. Results are shown in Figure 9. With the beam perpendicular to the sample chips, the reflections were circular with a strong (020) reflection and a weak (110) reflection. The circular shape indicated a random distribution of the *c* axes in the plane of the chip. When the sample was tilted 45° around its vertical axis, the (020) reflection disappeared in the equatorial region while the (110) reflection became more intense in that region. This behavior indicates a preferred crystallite orientation where the (100) planes are parallel to the substrate-coating interface with *c* axes randomly distributed in that plane.

From the above, one speculates that the substrate-coating interface determines the orientation of the crystals in the initial layer of particulates. Since the orientation measurements were made on coating chips 0.5–3 μm thick and the chips were composed of successively deposited 0.1-μm particulates, crystal growth in subsequent particles must have been governed by epitaxy. With some of the lower molecular weight oligomeric deposits, additional evidence of particle-particle transfer of crystallographic information was shown. In a separate experiment, a low molecular weight coating was deposited under the influence of a high electrostatic field. Analysis indicated low molecular weight acid chloride/hydrochloride compounds as well as diamine hydrochloride. SEMs of these deposits showed clear evidence of particle-particle transfer of information (Fig. 10). The coating deposit was in the form of columns which were composed of the characteristic 0.1-μm particles. The geometric shapes were clear indications

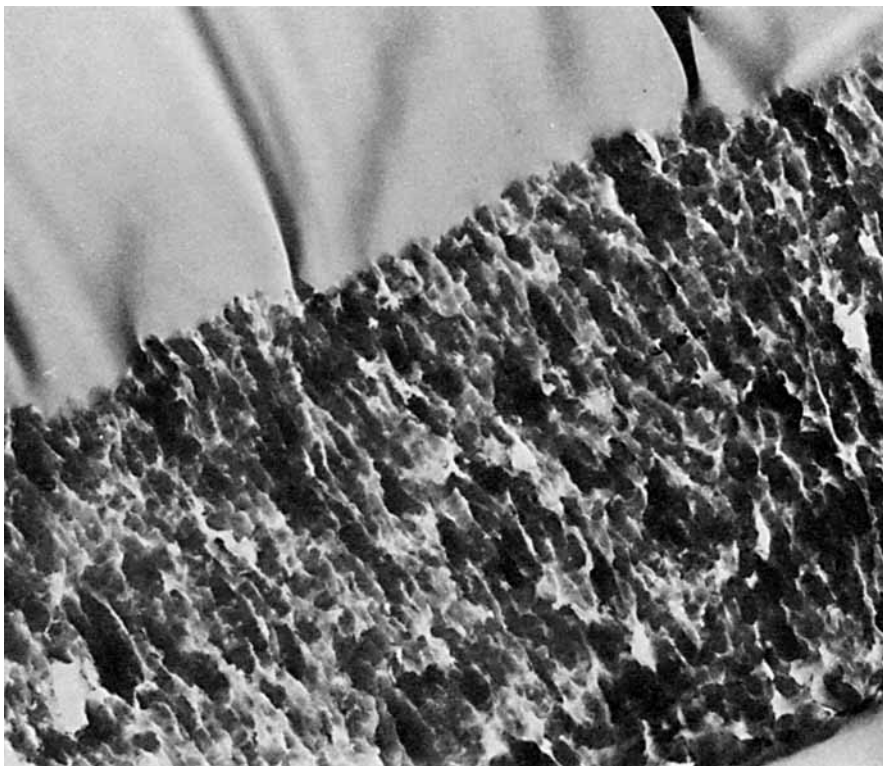
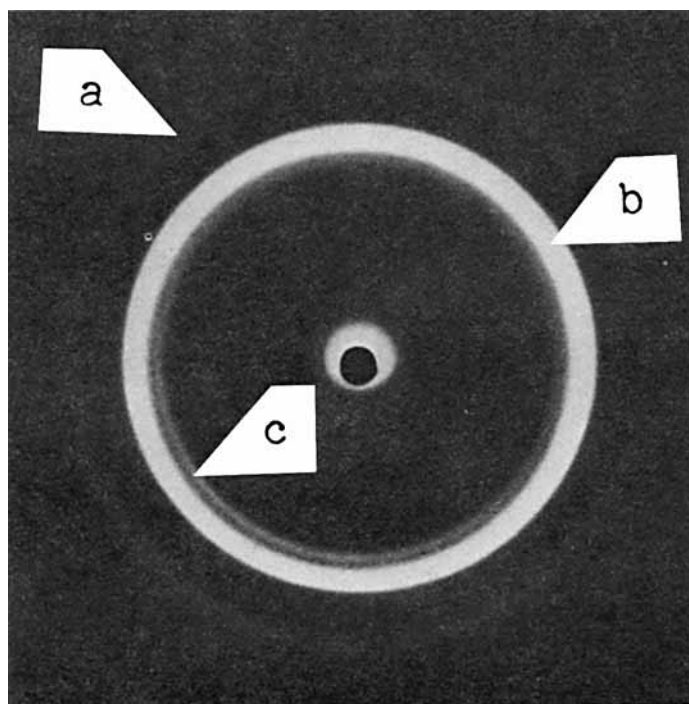


Fig. 8. Transmission electron micrograph of a cross section cut from a clear deposit made at 190°C.

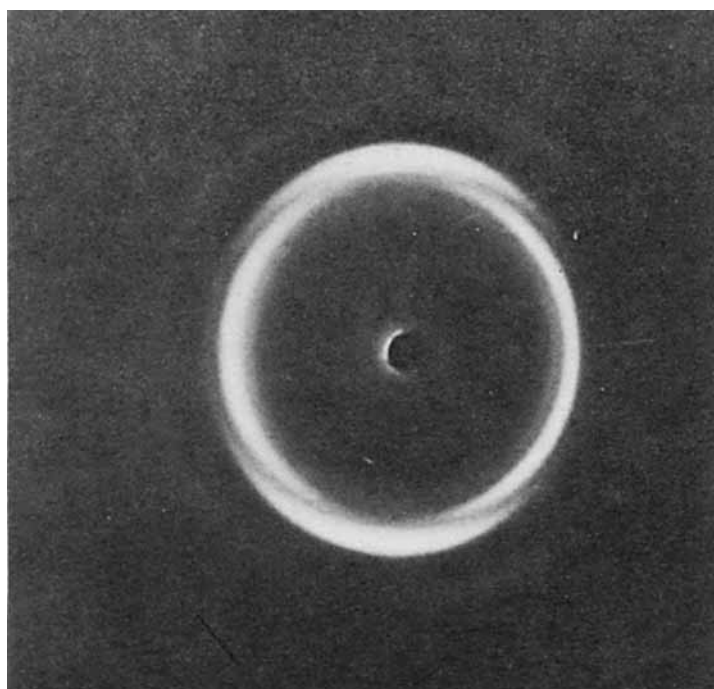
that crystal symmetry and orientation information could be transferred from particle to particle. The mechanism for this particle deposition/transport that would yield these deposits is not known.

Figure 11 shows an electron micrograph of a cross section of a hazy coating. The deformation and orientation of the small particles were not uniform, and holes were always found in the microtomed cross sections. This observation was in contrast to our experience with the clear coatings (Fig. 8), where the particles were always deformed uniformly by the cutting action. The nonuniformity of the particles was also accompanied by a lack of crystallite orientation with respect to the substrate surface. These observations, coupled with the finding that the hazy coatings were formed only at the higher monomer flow rates, lead to a possible mechanism of formation. One speculated that the higher monomer flow rates resulted in particle agglomeration in the gas phase with subsequent deposition of these larger agglomerates. This would account for the existence of the large mounds of particle agglomerates, and since there would be particle-particle contact prior to deposition, the particle-particle surfaces would govern the crystalline orientation. The agglomerates would take on the optical properties of a dendritic structure scattering light and thereby result in haze. This method of formation would also account for the lack of crystal orientation with respect to the coating surface, as well as the absence of deformation uniformity in the microtoming operation.

Combining the process information and the morphological observations, a



(a)



(b)

Fig. 9. X-ray flat-plate photographs made with clear, well-coalesced deposits on aluminum foil: (a) taken with the sample chips perpendicular to the x-ray beam; (b) taken with the chips rotated  $45^\circ$  about their vertical axes.

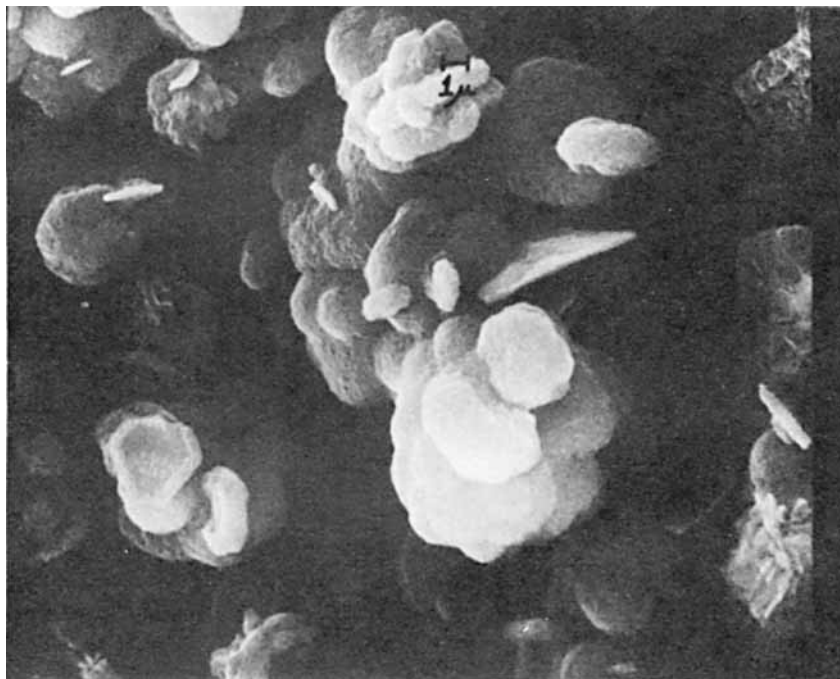


Fig. 10. Scanning electron micrograph of a low molecular weight, powdery deposit made under the influence of an electrostatic field.



Fig. 11. Transmission electron micrograph of a cross section cut from a hazy deposit made at 190°C.

mechanism for the formation of the vapor-deposited PPD-T coatings can be proposed. One speculates that the initial reaction of the monomers, PPD and TCl, took place in the gas phase. This initial reaction product—in reality an AB monomer—quickly condensed into a liquid droplet or semisolid particle, and the actual polymerization took place in this condensed, nongaseous phase. Such a sequence of events would account for the fact that high molecular weight polymer could be formed even with gross monomer imbalance (up to 2/1) in the gas phase. The condensed-phase nature of the polymerization would also account for the relatively high reaction rates actually observed. It is further assumed that the bulk of the polymerization and concurrent crystal formation probably took place after the particles were deposited. Since PPD-T is quite intractable even at very low molecular weights, partial polymerization and crystallization in the suspended particle would lead to a random crystal orientation in the coating deposits. This viewpoint was further supported by the observation that the molecular weight of the vapor-deposited PPD-T coatings was mostly dependent on the substrate temperature.

The reason for a minimum temperature for good polymer coating formation remains unclear. At least two factors, both temperature sensitive, are believed to be necessary for the solventless polymerization. First, monomer mobility is required for polymerization, and the 170°C temperature may represent the melting point of the initial PPD-TCl condensation product. A second possibility may involve the decomposition of the amine-hydrochloride condensation reaction product. The amine-hydrochloride must be destroyed for polymerization to proceed, and 170°C might be the minimum decomposition temperature for the elimination of HCl. We cannot distinguish between these two factors on the basis of our experiments.

The authors gratefully acknowledge the aid of R. G. Scott in obtaining the electron micrographs of the cross-sectioned coatings.

### References

1. H. Shin, U.S. Pat. 4,009,153 (1977).
2. R. J. Angelo, R. N. Blomberg, F. P. Boettcher, R. M. Ikeda, and M. R. Samuels, U.S. Pat. 4,104,438 (1978).
3. S. L. Kwolek, P. W. Morgan, and W. R. Sorenson, U.S. Pat. 3,063,966 (1962). T. I. Blair, P. W. Morgan, and F. L. Killian, *Polym. Prepr., Am. Chem. Soc., Div. Polym. Chem.*, **17**, 59 (1976).
4. F. B. Moody, private communication.
5. M. Salame and S. Steingiser, *Polym. Plast. Technol. Eng.*, **8**, 155 (1977).

Received May 7, 1979

Revised November 28, 1979